

Research article

UVA irradiation of riboflavin generates oxygen-dependent hydroxyl radicals

Saadettin Sel^{1,2,3}, Norbert Nass^{2,4}, Sandy Pöttsch⁵, Stefanie Trau², Andreas Simm^{5,6}, Thomas Kalinski⁴, Gernot IW. Duncker², Friedrich E. Kruse³, Gerd U. Auffarth¹, Hans-Jürgen Brömme⁶

¹Department of Ophthalmology, University of Heidelberg, Heidelberg, Germany, ²Department of Ophthalmology, Martin Luther University Halle Wittenberg, Halle (Saale), Germany, ³Department of Ophthalmology, University Erlangen-Nuremberg, Erlangen, Germany, ⁴Institute for Pathology, Otto-von-Guericke-University, Magdeburg, Germany, ⁵Department of Thoracic Surgery, Martin Luther University Halle Wittenberg, Halle (Saale), Germany, ⁶Center for Medical Basic Research of the Medical Department, Martin-Luther-University Halle-Wittenberg, Halle (Saale), Germany

Objectives/methods: The aim of this study was to verify the formation of hydroxyl radicals ($\cdot\text{OH}$) after ultraviolet A (UVA) irradiation of riboflavin (RF) by spin trapping with 5,5-dimethyl-1-pyrroline-*N*-oxide (DMPO), and electron spin resonance spectroscopy.

Results: We found that $\cdot\text{OH}$ were generated via hydrogen peroxide (H_2O_2) formation during UVA irradiation of RF. The $\cdot\text{OH}$ radicals were trapped with DMPO yielding 2-hydroxy-5,5-dimethyl-1-pyrroline-*N*-oxide ($\cdot\text{DMPO-OH}$). The formed radical adduct ($\cdot\text{DMPO-OH}$) accumulated in the RF solution. Argon equilibration of the RF solution completely blocked the formation of the $\cdot\text{DMPO-OH}$ adduct whereas subsequent aeration restored radical adduct generation. The presence of catalase inhibited $\cdot\text{DMPO-OH}$ generation whereas BSA had no influence on $\cdot\text{DMPO-OH}$ formation. Stopping UVA irradiation led to decay of radical adducts. UVA irradiation of H_2O_2 in the presence of DMPO but without RF also induced the formation of $\cdot\text{DMPO-OH}$ adduct. When adding DMPO to an already irradiated RF solution significantly less $\cdot\text{DMPO-OH}$ was formed during further irradiation. Ultraviolet-visible spectroscopy and high-performance liquid chromatography analysis of RF indicated that RF decayed during UVA irradiation.

Discussion: The formation of $\cdot\text{OH}$ during UVA irradiation of RF may be part of the oxygen-dependent mechanism involved in the cross-linking therapy of collagen in corneal stroma.

Keywords: UVA, Riboflavin, Electron spin resonance, 5, 5-Dimethyl-1-pyrroline *N*-oxide, Spin trapping, Hydroxyl radical, Hydrogen peroxide, Catalase, UV-VIS spectroscopy, High-performance liquid chromatography

Introduction

Corneal collagen cross-linking (CXL) therapy for patients with keratoconus is a technique that exploits a combination of ultraviolet A (UVA) light and riboflavin (RF) to induce cross-linking of collagen and thereby increases the stability of corneal stroma.¹⁻³ This treatment method works by improving the biomechanical properties of corneal tissue and by increasing its resistance to enzymatic digestion.⁴⁻⁶ Despite the vast clinical knowledge on the beneficial therapeutic effects of CXL, the exact molecular mechanisms of cross-linking are largely unknown. Recently, it has

been reported that carbonyl groups and reactive oxygen species are essential to cross-linking.⁷

Concerning the possible molecular mechanism leading to the cross-linking of collagen, some authors favor singlet oxygen ($^1\text{O}_2$) as the prevailing oxidant^{5,8} which is based on the ability of sodium azide or dimethylsulphoxide to inhibit the reactivity of the photo-excited RF.⁵ Kamaev *et al.* underlined the role of RF triplets and reactive groups of corneal proteins in the cross-linking of the proteins through radical reactions.⁹

In this study, spin trapping technique in combination with electron spin resonance (ESR) spectroscopy was used to demonstrate oxygen-dependent generation of hydroxyl radicals by UVA irradiation of RF. The formation of hydroxyl radicals involves

Correspondence to: Saadettin Sel, Department of Ophthalmology, University of Heidelberg, Im Neuenheimer Feld 400, D-69120 Heidelberg, Germany. Email: saadettinsel@googlemail.com

The first two authors contributed equally to this work.

the intermediate generation of hydrogen peroxide (H_2O_2).

Material and methods

Chemicals and instruments

5,5-Dimethyl-1-pyrroline-*N*-oxide (DMPO), H_2O_2 (30% w/w), catalase from bovine liver, and bovine serum albumin (BSA) were purchased from Sigma-Aldrich Chemie GmbH (Munich, Germany) and isotonic sodium chloride solution (0.9% NaCl) from Baxter (Unterschleissheim, Germany). RF solution was obtained from Streuli Pharma AG (Uznach, Switzerland). This RF solution is in clinical use for CXL treatment and consists of 5 mg RF in 1 ml NaCl (0.154 M). Argon gas 4.8 was purchased from Linde AG (Leuna, Germany). Acetonitrile (HPLC Ultra-gradient grade) and trifluoroacetic acid were obtained from Carl Roth GmbH (Karlsruhe, Germany).

The ESR spectrometer (MS-100) was manufactured by Magnettech GmbH (Berlin, Germany), the HPLC-equipment (Series 1200) was from Agilent Technologies (Waldbronn, Germany) and the ultraviolet-visible (UV-VIS) spectrophotometer (Specord S600) was obtained from Analytik Jena (Jena, Germany). The quartz cuvette (1.5 ml) was obtained from Hellma GmbH & Co. KG (Muehlheim, Germany), the UVA diodes were purchased from Roithner Laser Technik (Vienna, Austria), and the ESR capillaries were obtained from VWR (Dresden, Germany).

UVA irradiation of riboflavin

RF and DMPO were dissolved in 0.9% NaCl solution (RF solution: 300 μl of 13.3 mM RF (final concentration 4 mM) and 100 μl of 1 M DMPO (final concentration 0.1 M) dissolved in 600 μl of 0.154 M NaCl). This RF solution was air-saturated and irradiated by UVA in a stirred quartz cuvette for up to 90 minutes at room temperature (Fig. 1). Ambient temperature was used since our ESR-spectrometer did not have a temperature controlled unit. Two UV-LED 5 mm diodes (370 ± 15 nm), fixed in front of the cuvette were used for irradiation. An irradiance of the RF solution with $3.0 \text{ mW}/\text{cm}^2$ was adjusted which is also used clinically for CXL treatment. Fifty microlitres of aliquots from the RF solution were transferred from the stirred quartz cuvette into a small glass capillary for the subsequent ESR-analysis, before as well as 1, 5, 10, 20, 30, 40, 50, 60, 70, and 90 minutes after starting UVA irradiation. Constant stirring of the content of the cuvette guaranteed a widely uniform illumination of the mixture and should prevent inhomogeneity.

When necessary, the sample could be purged via a needle in the lid of the cuvette holder by air or by argon gas. Equilibration of the RF solution with

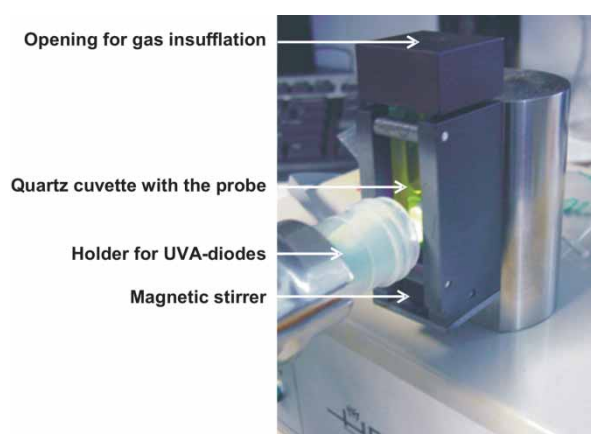


Figure 1 UVA irradiation unit. A stirred quartz cuvette containing the sample is positioned in a black metal chamber having an opening only towards the site of UVA-illumination. The experiments were carried out in a darkened room at room temperature. The sample is irradiated by two UVA diodes (370 ± 15 nm) with $3.0 \text{ mW}/\text{cm}^2$. Constant stirring of the mixture largely prevented an inhomogeneous distribution of RF in the cuvette. The sample can be purged on demand via a needle in the lid of the cuvette holder by air or by argon gas.

argon started 15 minutes before irradiation and continued during UVA illumination by gently bubbling with argon gas. Re-equilibration of the sample with oxygen was achieved by purging the mixture with air. Catalase or BSA (each 170 μg protein/ml as final concentration) was added just prior to UVA irradiation. In another set of experiments illumination of RF was stopped after 10 minutes. The adduct content ($\cdot\text{DMPO-OH}$) was traced for further 80 minutes. To analyze the stability of RF under UVA irradiation, we extended the illumination time for up to 5 hours without DMPO present. DMPO was added after this illumination period to determine the ability of residual RF to form radicals.

ESR spectroscopy

Fifty microlitres of aliquots of the RF solution were transferred into a small glass capillary before or 1, 5, 10, 20, 30, 40, 50, 60, and 90 minutes after starting irradiation in the quartz cuvette. The capillary was sealed with plasticine and immediately put into the cavity of an ESR spectrometer. A back diffusion of oxygen into the ESR capillary during the 2-minute recording period appears to be unlikely. The second band (Fig. 2) of the ESR spectrum was used for measuring the relative ESR signal intensity of the $\cdot\text{DMPO-OH}$ (2-hydroxy-5,5-dimethyl-1-pyrroline-*N*-oxide) adduct (relative ESR signal intensity) by means of arbitrary units (a.u.). The following ESR settings were adjusted for the measurements: center field: 3370 G, sweep width: 100 G, sweep time: 120 seconds, number: 1, modulation amplitude: 0.1 G, power attenuation: 6 dB, receivers gain: 50. Each experiment was repeated five times and the data expressed as

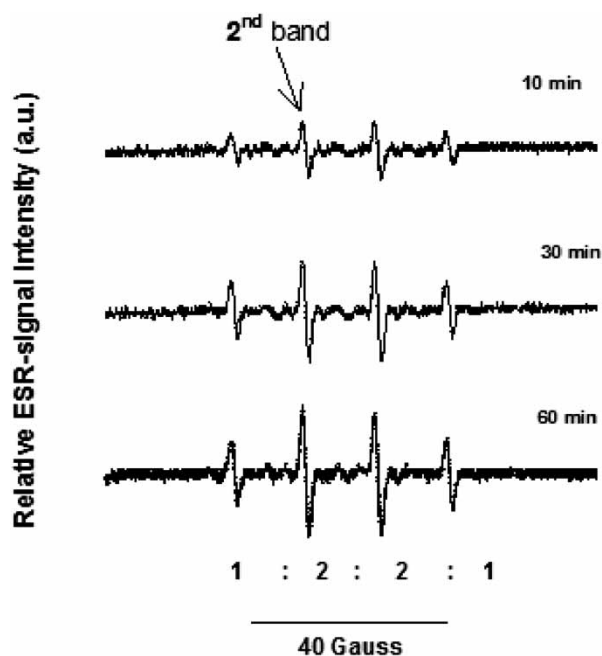


Figure 2 ESR spectra of the \cdot DMPO-OH adduct detected during UVA irradiation of RF. ESR spectra were recorded during UVA illumination of RF in the presence of DMPO dissolved in isotonic NaCl (4 mM RF and 0.1 M DMPO dissolved in 1 ml of 0.154 M NaCl (0.9%)). Fifty microliters of aliquots were taken from the RF solution before and during irradiation at different time points (for more clarity only spectra taken after the 10th, 30th and 60th minutes were displayed). The characteristic ESR spectrum of the \cdot DMPO-OH adduct (1:2:2:1) was measured in an ESR spectrometer at following spectrometer settings: center field 3370 G, sweep width 100 G (10 mT), sweep time 120 seconds, number 1, modulation amplitude 100 mG, power attenuation 6 dB, receiver gain 50. The second band of the ESR spectrum was used as a measure for the relative ESR signal intensity of the \cdot DMPO-OH adduct which is expressed in arbitrary units (a.u.).

mean \pm standard error of the mean. These results were plotted against time.

Ultraviolet-visible spectroscopy

The entire cuvette containing 25 μ g RF in 0.154 mM NaCl (total volume of 1.0 ml) was transferred from the place of irradiation (Fig. 1) to the spectral photometer (before and after 30, 60, 90, 120, 150, and 180 minutes UVA irradiation). The spectra were recorded between 200 and 550 nm at room temperature. Each measurement took less than 0.5 minutes. Thereafter the cuvette was placed again in front of the UVA diodes to continue irradiation. A limited entry of oxygen during this cuvette transfer cannot be excluded.

High-performance liquid chromatographic analysis

High-performance liquid chromatographic (HPLC) analysis of RF and its UVA-modified derivatives was performed on a HPLC system (Series 1200) from Agilent Technologies. The system consisted of a

vacuum degasser, a quaternary pump unit, an autosampler for sample injections, a thermostated column compartment, and a photodiode array (detector (DAD) for peak analysis within a wavelength range of 200–550 nm). The analytical column (Zorbax Eclipse XDB-C18, 4.6 \times 150 mm, particle size 5 μ m Agilent, Waldbronn, Germany) was used for sample separation.

The mobile phase gradient consisted of 0% acetonitrile/0.1% TFA in water (0 minute) and 100% acetonitrile/0.1% TFA (20 minutes). Five microliters of the sample (25 μ g RF/ml) was injected by the autosampler. The separations were run at 30°C with a flow rate of 0.5 ml/minute. The chromatogram was recorded at 254 nm.

Results

To investigate whether hydroxyl radicals (\cdot OH) are formed by UVA irradiation of RF, we applied the nitron spin trap DMPO and ESR. With this technique, we could confirm the generation of \cdot OH by the characteristic 1:2:2:1 ESR spectrum of the \cdot DMPO-OH adduct (Fig. 2). Radical adduct (\cdot DMPO-OH) intensity rose within the first 30–40 minutes of UVA irradiation of RF before reaching a maximum. The formation of \cdot OH required the presence of oxygen since its displacement by argon blocked the radical adduct generation whereas re-equilibration with air restored radical adduct formation (Fig. 3). RF-derived \cdot OH formation involved the

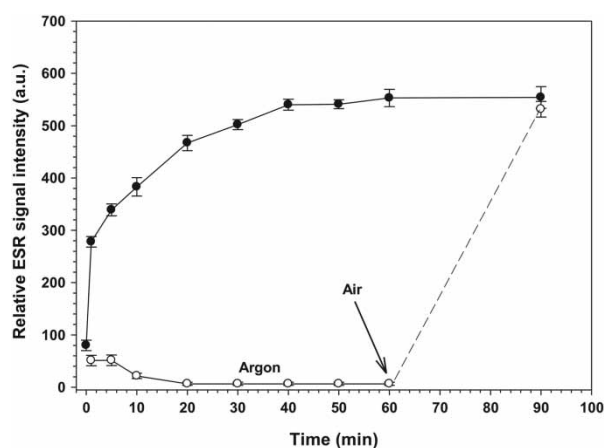


Figure 3 Relative ESR signal intensity of the \cdot DMPO-OH adduct in the presence of air or argon. RF solution (c was stirred vigorously under air (filled circles) or purged with argon gas for 15 minutes (open circles) thereafter UVA irradiation (3.0 mW/cm²) was started at room temperature. For recording the ESR spectrum, 50 μ l of aliquots were taken from the RF solution before and during UVA irradiation (0, 1, 5, 10, 20, 30, 40, 50, 60, and 90 minutes). Each experiment was repeated independently five times. The intensity of the second band of the \cdot DMPO-OH adduct spectrum was determined and plotted against time. The results are expressed as mean of the relative ESR signal intensity and the error bars show the SEM.

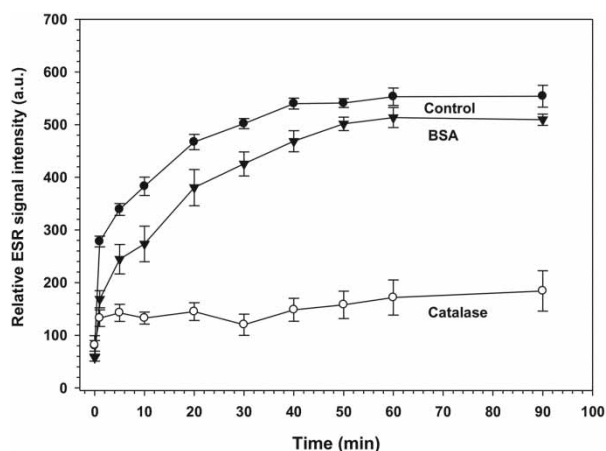


Figure 4 Influence of catalase on relative ESR signal intensity of the \cdot DMPO-OH adduct. Sample composition and ESR settings correspond to those described in Fig. 3. Additionally, either 170 μ g catalase (open circles) or 170 μ g BSA (triangles) were added. The data for each group at each time point represent the mean of five experiments. Standard error is presented by error bars.

generation of H_2O_2 since addition of catalase significantly diminished the radical adduct signal. Addition of BSA instead of catalase decreased the development of the radical adduct only marginally (Fig. 4). UVA irradiation of H_2O_2 and DMPO in the absence of RF produced also the \cdot DMPO-OH adduct, indicating the ability of UVA to cleave H_2O_2 photo-chemically into two \cdot OH radicals. UVA irradiation of DMPO without RF and H_2O_2 does not form any radical adduct (Fig. 5).

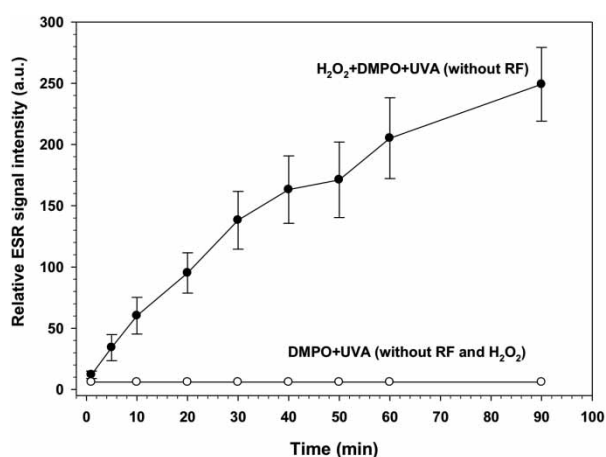


Figure 5 UVA irradiation of hydrogen peroxide in the absence of RF. DMPO (0.1 M) dissolved in 1 ml NaCl solution (0.9%) was irradiated by UVA-light in the presence (filled circles) or absence (open circles) of hydrogenperoxide (0.65 mM). UVA irradiation and sample preparation for ESR analysis as well as ESR spectrometer settings were according to Fig. 3. Each data point (filled circles) represents the mean value of five experiments of ESR signal intensity of the \cdot DMPO-OH adduct with error bars representing the SEM. In the experiments with the DMPO solution only (open circles), the ESR signal intensities were almost undetectable.

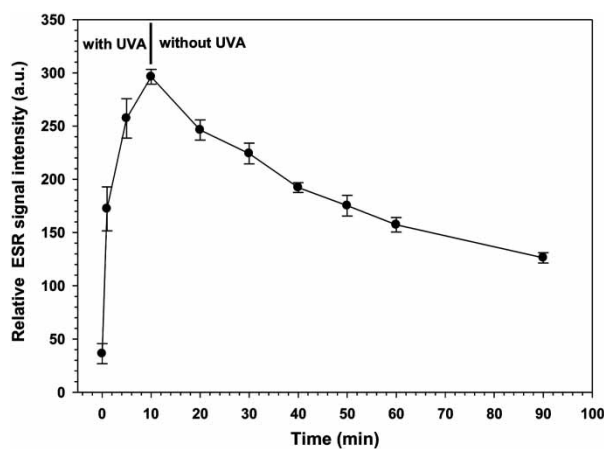


Figure 6 Effect on relative ESR signal intensity of \cdot DMPO-OH adduct after stopping the UVA irradiation of RF. The RF solution, sample collection at each time point as well as the UVA irradiation and ESR settings are described for the experiments in Fig. 3. UVA irradiation of the RF solution was stopped after 10 minutes.

Immediately after stopping UVA irradiation of the RF solution, ESR signal intensities of \cdot DMPO-OH adduct spectra began to decline (Fig. 6) suggesting that only during UVA irradiation of RF hydroxyl radicals are generated. Consistently, if DMPO was incubated in the presence of H_2O_2 and RF in a non-illuminated cuvette no detectable adduct was produced (not shown).

To evaluate the effect of prolonged illumination by UVA on the integrity of RF molecule, RF containing solution was subjected to UVA irradiation for 5 hours in the presence of oxygen, which was achieved by

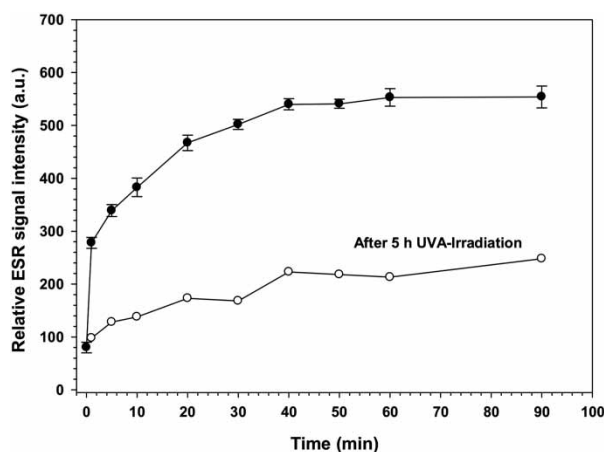


Figure 7 Effect on relative ESR signal intensity of \cdot DMPO-OH adduct after UVA irradiation of RF for 5 hours. RF solution (4.43 mM RF in 0.9 ml of 0.154 M NaCl (0.9%)) was irradiated with UVA (370 nm, 3.0 mW/cm²) for 5 hours. Thereafter 100 μ l of 1 M DMPO was added as spin trap to the solution (open circles) and under continued UVA illumination 50 μ l samples were taken for ESR analysis at different time points. For controls, RF solution (4 mM RF and 0.1 M DMPO dissolved in 1 ml of 0.154 M NaCl (0.9%)) (filled circles) was prepared shortly before starting the UVA irradiation (filled circles).

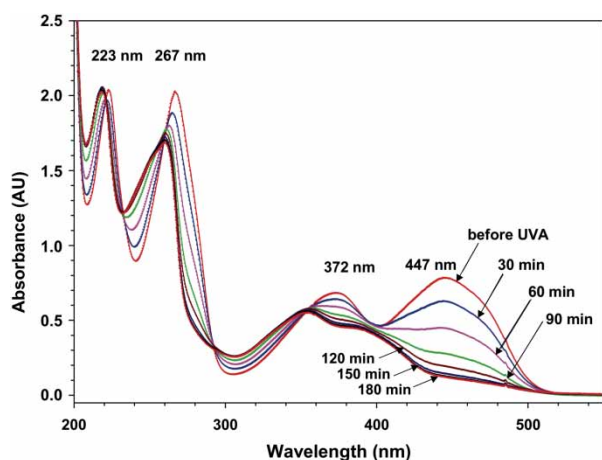


Figure 8 Influence of UVA irradiation on UV-VIS spectra of RF. One milliliter of RF solution (0.067 mM) in NaCl (0.154 M) was irradiated with UVA under continuous stirring in the presence of oxygen. The whole cuvette was relocated before and after 30, 60, and 90 minutes UVA irradiation to a spectrophotometer to record the spectrum between 200 and 550 nm. Thereafter the cuvette was relocated to the UVA irradiation unit. The absorbance is given in absorbance units (a.u.).

occasionally purging of the cuvette with air. Then DMPO was added as spin trap to the solution and exposure to UVA was continued for further 90 minutes. ESR analysis revealed that previous extended UVA irradiation decreased significantly the ability of RF to form $\cdot\text{DMPO-OH}$ adduct (Fig. 7). To further assess this UVA-induced decay of RF, we performed UV-VIS spectroscopy (Fig. 8) and HPLC analysis (Fig. 9). In the UV-VIS spectra, the absorbance at 445 nm primarily decreased with irradiation time (Fig. 8).

In HPLC chromatograms (Fig. 9A) the peaks 1–4 appeared to be RF and its derivatives, based on their UV-VIS spectra (comparison of Fig. 8 with Fig. 9B). Peak 5 was not RF but originated from it (Fig. 9C) since UVA irradiation of RF decreased the peak area of RF (mostly of peak 2) and increased area of peak 5. UVA irradiation altered primarily RF-absorption at 445 nm which disappeared with prolonged UVA irradiation and was lost after 30 minutes of illumination (Fig. 9C). After 120 minutes of UVA irradiation, peak 2 was almost completely degraded, whereas peak 5 increased significantly.

Discussion

In this study, we demonstrated that UVA irradiation of RF generated hydroxyl radicals ($\cdot\text{OH}$) which were immediately trapped by DMPO giving a radical adduct that showed a characteristic quartet of ESR signals with an intensity ratio of 1:2:2:1.^{10,11} Thus, we were able to monitor the formation of this radical adduct time-dependently by ESR spectroscopy. Radical adduct formation needed both, the presence

of dissolved oxygen as well as the photosensitizer RF in the irradiated sample. Substitution of oxygen by argon blocked radical adduct formation whereas re-equilibration of the sample with air reconstituted its production. Obviously, in this reaction, molecular oxygen is stepwise reduced via the superoxide radical anion ($\cdot\text{O}_2^-$) to H_2O_2 . The formation of H_2O_2 by irradiation of RF with polychromatic light has been convincingly demonstrated by Silva *et al.*¹² and by Sato *et al.*¹³ In our experimental setup H_2O_2 appears to be a necessary intermediate towards $\cdot\text{OH}$ formation, since the presence of catalase diminished the amount of radical adduct formed. In contrast to catalase, BSA as a control protein only marginally influenced the amount of radical adduct formation, demonstrating that catalase acted specifically via degradation of H_2O_2 .

If we assume that H_2O_2 is formed during UVA irradiation of RF by stepwise reduction of oxygen, H_2O_2 should be simultaneously split by UVA in two hydroxyl radicals. The results shown in Fig. 5 demonstrated that UVA was indeed capable to split H_2O_2 in the absence of RF and the resulting $\cdot\text{OH}$ radicals were trapped by DMPO to form $\cdot\text{DMPO-OH}$ adducts whereas in the absence of H_2O_2 , radical adduct formation was completely absent.

As long as sufficient RF and oxygen were available, we expected that the amount of radical adduct should constantly rise during sample illumination. However, in our experiments, the adduct formation reached a maximal level after about 30–40 minutes of irradiation. The existence of such a plateau in the radical adduct intensity appears to be caused by a steady state equilibrium between a continuously UVA-triggered generation of $\cdot\text{OH}$ from RF and a simultaneously ongoing decay of the radical adduct. Stopping UVA irradiation and thus stopping the formation of $\cdot\text{OH}$ immediately resulted in a decline in the radical adduct intensity. Indeed, it has been reported that the $\cdot\text{DMPO-OH}$ adduct is unstable and decays with a half-life of about 20–25 minutes at room temperature.^{14,15} Additionally, RF concentration was reduced by approximately 30% after 30-minute illumination (Fig. 9) and this also contributed to a decreased formation of radical formation.

However, the formation of the DMPO-OH adduct after UVA illumination of RF in the presence of DMPO might also be explained by another pathway. It is well established that the DMPO-OH adduct can result from the decay of the superoxide radical adduct.^{16,17} This reaction can take place without the intermediate formation of H_2O_2 as we proposed. It could even explain the time dependence of the formation of the DMPO-OH adduct originating from the intermolecular rearrangement of one adduct into the other. However, it does not explain the action of

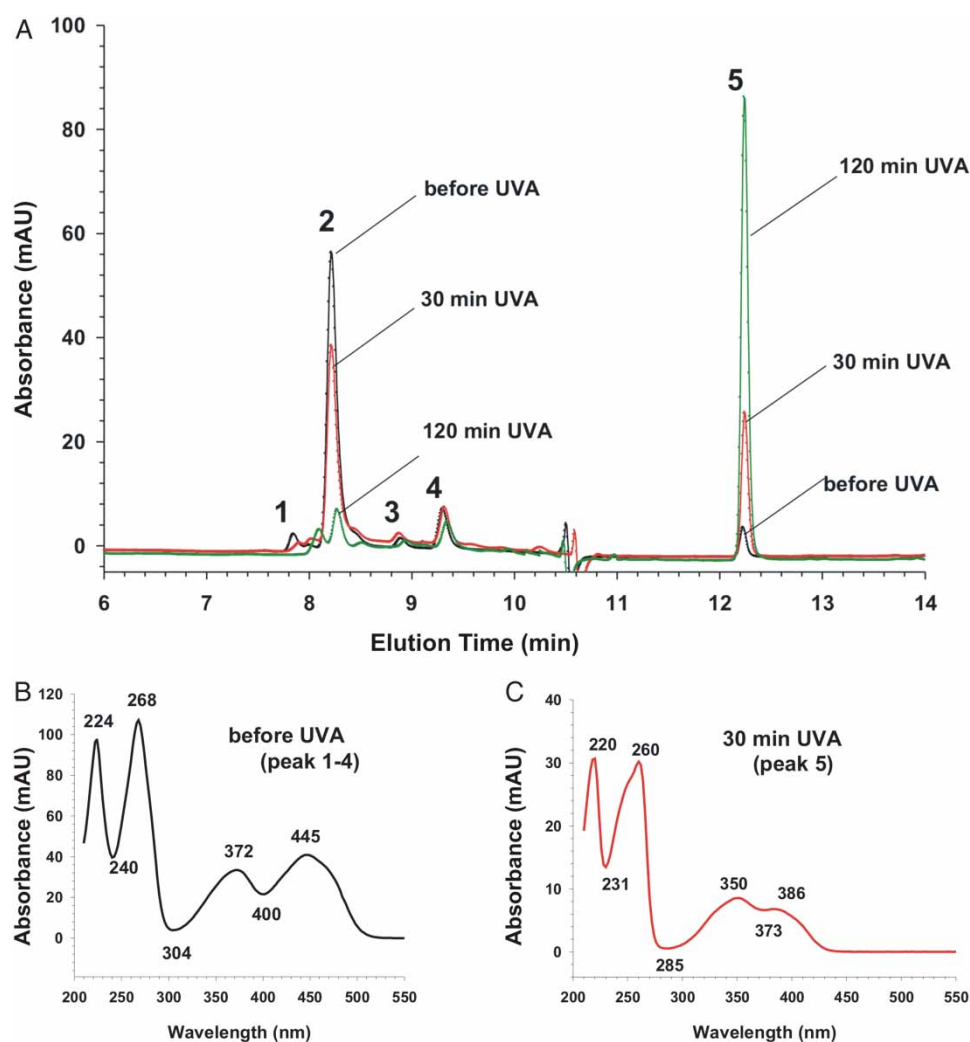


Figure 9 HPLC analysis of RF reaction mixture during UVA irradiation. (A) HPLC chromatograms (absorption at 254 nm) of 5 μ l of aliquots of the RF-containing sample (25 μ g RF/ml). Black chromatogram represents the reaction mixture before irradiation and red and green curves after 30- and 120-minute irradiation, respectively. Peaks were numbered from 1 to 5 according to elution time. The absorption peaks 1, 2, 3, and 4 (peak 1–4) have all the same UV-VIS spectrum, which is representatively shown in (B) from the peak 2. The UV-VIS spectrum of peak 5 is shown in (C) which is similar to UV-VIS spectrum of RF after UVA irradiation as in Fig. 8. The absorbance area of peak 2 diminishes whereas the absorbance area of peak 5 increases during UVA irradiation of the RF sample.

catalase in preventing the formation of the DMPO-OH adduct. Another well-known alternative way of DMPO-OH formation is the so-called Fenton-reaction. This type of DMPO-OH generation needs beside H_2O_2 the additional presence of ferrous iron (Fe^{2+}) or other transition metal ions like Cu^+ . It cannot be completely excluded that traces of such a catalytically active transition metal ion were accidentally introduced from the other ingredients of the illuminated mixture. Usually, the simultaneous presence of ferrous iron and H_2O_2 induces an immediate generation of hydroxyl radicals which form DMPO-OH adducts detectable by ESR spectroscopy within seconds. Hydroxyl radical formation by the Fenton-reaction stops when ferrous iron is oxidized to ferric iron. The time-dependent formation of the adduct, as observed in our experiments, might be conceivable if the ferric iron ions are continuously re-reduced by

superoxide anion radicals. This possibility cannot be completely excluded. However, when we incubated RF and DMPO and H_2O_2 without illumination in controls, no detectable DMPO-OH signal was generated (data not shown). If accidentally introduced ferrous iron ions were present, we would expect that the Fenton reaction would be capable to produce at least a small signal.

Another possible pathway of adduct formation has been described by Ueda *et al.*¹⁷ These authors demonstrated that the formation of singlet oxygen by UVA (330 nm) irradiation of hematoporphorin in the presence of phenolic compounds and DMPO gave an ESR spectrum characteristic of $\cdot\text{DMPO-OH}$. According to their results, singlet oxygen reacts first with DMPO, and the resulting $\text{DMPO-}^1\text{O}_2$ intermediate is immediately decomposed/reduced in the presence of phenolic compounds to give $\cdot\text{OH}$. In contrast

to our results, the maximum of adduct accumulation was achieved already after two seconds of irradiation and the presence of catalase had little effect on signal intensity of $\cdot\text{DMPO-OH}$. This indicates that the formation of $\cdot\text{OH}$ is not mediated by H_2O_2 under the conditions used by Ueda *et al.*¹⁷

It has been demonstrated that the absorption spectra of RF is changing after different time intervals of UVA irradiation.¹⁸ We were able to confirm this result (Figs. 8 and 9). When RF was continuously irradiated for several hours and thereafter the spin trap DMPO was added to the still illuminated sample, radical adduct formation was remarkably reduced. It is well known that RF is destroyed or transformed during irradiation^{18,19} and thus apparently less H_2O_2 and fewer $\cdot\text{OH}$ was generated after addition of DMPO. In this experiment, the irradiated sample was purged gently with air to avoid depletion of oxygen.

HPLC analysis performed after different time intervals of RF-irradiation also confirmed the assumption that RF was destroyed or transformed during UVA irradiation. The non-irradiated RF eluted from the column after 8.3 minutes (peak 2). This peak declined with proceeding illumination. A product peak (peak 5) was formed during UVA treatment. It was eluted from the column at 12.2 minutes. This peak (peak 5) increased during UVA treatment demonstrating a continuous shift from native RF to a product losing its ability to form $\cdot\text{OH}$ by UVA irradiation. The two major products of photodegradation of RF appear to be lumichrome and lumiflavin as shown previously.^{19,20} The observed UV-absorption maximum (350 nm) of peak 5 in Fig. 9 demonstrates that under the conditions used by us lumichrome appears to be the main product of RF degradation.

Despite the fact that corneal collagen cross-linking therapy for progressive keratoconus using UVA of 370 nm wavelength and RF has been shown to be quite effective, the precise molecular mechanisms of cross-linking are mostly unknown.⁷ Our experimental setup as well as the used analytic equipment (ESR spectroscopy) did not allow a direct observation of the formation of singlet oxygen ($^1\text{O}_2$). Thus, we cannot evaluate the individual impacts of both strongly oxidizing species ($^1\text{O}_2$ and $\cdot\text{OH}$) regarding their ability to induce corneal cross-linking of collagen.

The effect of photo-excited RF on the viscosity of hyaluronic acid solutions was investigated by Frati *et al.*⁵ The authors could demonstrate that UV irradiation of RF under aerobic conditions caused fragmentation of hyaluronic acid and a decrease in the viscosity of its solutions. They concluded that the most likely chemical species involved in the reaction is the hydroxyl radical. Furthermore, it is well

established from other investigations that $\cdot\text{OH}$ radicals are able to modify amino acids and to cleave peptide bonds in proteins^{21–24} and participate in diverse cross-linking reactions²⁵ In other studies it could be shown that irradiation of RF by UVA induces damage of DNA-base pairs.^{26–29}

Illumination of several photosensitizers in aqueous solution produces $\cdot\text{O}_2^-$, H_2O_2 and $\cdot\text{OH}$ in addition to $^1\text{O}_2$.^{14,30–33} According to the above-mentioned radicals and $^1\text{O}_2$, Kamaev *et al.*⁹ showed that the formation of RF-derived radicals might be also involved in cross-linking of corneal proteins. Therefore, it cannot be assumed that $^1\text{O}_2$ is the only species responsible for any damage/modification observed.⁸ But, vice versa, it can also not be excluded that the formation of $\cdot\text{DMPO-OH}$ might be only a consequence of an interaction of $^1\text{O}_2$ with DMPO and of the subsequent decay of the intermediate complex to form DMPO-OH and free $\cdot\text{OH}$. If the half-lives of $\cdot\text{OH}$ and $^1\text{O}_2$ in cells are compared with each other it is obvious that the half-life of $\cdot\text{OH}$ (10^{-9} s) is several times shorter than those of the $^1\text{O}_2$ (10^{-6} s).³³ The very short half-life of the $\cdot\text{OH}$ underlines its extraordinary high reactivity and makes it a substantial additional candidate for cross-linking of collagen. In conclusion, our ESR spectroscopic experiments demonstrated that during illumination of RF with UVA beside H_2O_2 , reactive hydroxyl radicals were produced. Whether these strongly oxidizing $\cdot\text{OH}$ are involved in cross-linking of collagen can currently not be answered and needs further studies.

Nevertheless, a deeper understanding of the radical-chemistry of collagen cross-linking by UVA and RF might lead to the development of alternative procedures that do not involve potentially harmful procedures like the abrasion of the epithelium or long term illumination with UVA-light.

Acknowledgment

We would like to thank Dr Hendrik Metz (Institute of Pharmacy of the Martin-Luther-University, Halle-Wittenberg, Germany) for assessment of ESR experiments.

Funding

This work was supported by Wilhelm Roux Program grant from Martin Luther University Halle-Wittenberg.

References

- 1 Spoerl E, Huhle M, Seiler T. Induction of cross-links in corneal tissue. *Exp Eye Res* 1998;66:97–103.
- 2 Wollensak G, Iomdina E, Dittert DD, Salamatina O, Stoltz G. Cross-linking of scleral collagen in the rabbit using riboflavin and UVA. *Acta ophthalmologica Scandinavica* 2005;83:477–82.

- 3 Wollensak G, Spoerl E, Seiler T. Riboflavin/ultraviolet-a-induced collagen crosslinking for the treatment of keratoconus. *Am J Ophthalmol* 2003;135:620–27.
- 4 Spoerl E, Wollensak G, Seiler T. Increased resistance of cross-linked cornea against enzymatic digestion. *Curr Eye Res* 2004;29:35–40.
- 5 Frati E, Khatib AM, Front P, Panasyuk A, Aprile F, Mitrovic DR. Degradation of hyaluronic acid by photosensitized riboflavin in vitro. Modulation of the effect by transition metals, radical quenchers, and metal chelators. *Free Radic Biol Med* 1997;22:1139–44.
- 6 Wollensak G, Iomdina E. Long-term biomechanical properties of rabbit sclera after collagen crosslinking using riboflavin and ultraviolet A (UVA). *Acta Ophthalmol* 2009;87:193–8.
- 7 Brummer G, Littlechild S, McCall S, Zhang Y, Conrad GW. The role of nonenzymatic glycation and carbonyls in collagen cross-linking for the treatment of keratoconus. *Invest Ophthalmol Vis Sci* 2011;52:6363–9.
- 8 Martin JP, Logsdon N. The role of oxygen radicals in dye-mediated photodynamic effects in *Escherichia coli* B. *J Biol Chem* 1987;262:7213–9.
- 9 Kamaev P, Friedman MD, Sherr E, Muller D. Photochemical kinetics of corneal cross-linking with riboflavin. *Invest Ophthalmol Vis Sci* 2012;53:2360–7.
- 10 Finkelstein E, Rosen GM, Rauckman EJ. Spin trapping of superoxide and hydroxyl radical: practical aspects. *Arch Biochem Biophys* 1980;200:1–16.
- 11 Yamazaki I, Piette LH. ESR spin-trapping studies on the reaction of Fe²⁺ ions with H₂O₂-reactive species in oxygen toxicity in biology. *J Biol Chem* 1990;265:13589–94.
- 12 Silva E, Edwards AM, Pacheco D. Visible light-induced photo-oxidation of glucose sensitized by riboflavin. *J Nutr Biochem* 1999;10:181–5.
- 13 Sato H, Taguchi H, Maeda T, Minami H, Asada Y, Watanabe Y, Yoshikawa K. The primary cytotoxicity in ultraviolet-A-irradiated riboflavin solution is derived from hydrogen peroxide. *J Invest Dermatol* 1995;105:608–12.
- 14 Taira J, Mimura K, Yoneya T, Hagi A, Murakami A, Makino K. Hydroxyl radical formation by UV-irradiated epidermal cells. *J Biochem* 1992;111:693–5.
- 15 Sankuratri N, Kotake Y, Janzen EG. Studies on the stability of oxygen radical spin adducts of a new spin trap: 5-methyl-5-phenylpyrroline-1-oxide (MPPPO). *Free Radic Biol Med* 1996;21:889–94.
- 16 Roubaud V, Sankarapandi S, Kuppusamy P, Tordo P, Zweier JL. Quantitative measurement of superoxide generation using the spin trap 5-(diethoxyphosphoryl)-5-methyl-1-pyrroline-N-oxide. *Anal Biochem* 1997;247:404–11.
- 17 Ueda J, Takeshita K, Matsumoto S, Yazaki K, Kawaguchi M, Ozawa T. Singlet oxygen-mediated hydroxyl radical production in the presence of phenols: whether DMPO-^{*}OH formation really indicates production of ^{*}OH? *Photochem Photobiol* 2003;77:165–70.
- 18 Hasan N, Ali I, Naseem I. Photodynamic inactivation of trypsin by the aminophylline-riboflavin system: involvement of hydroxyl radical. *Med Sci Monit* 2006;12:BR283–9.
- 19 Buettner GR. The spin trapping of superoxide and hydroxyl free radicals with DMPO (5,5-dimethylpyrroline-N-oxide): more about iron. *Free Radic Res Commun* 1993;19(Suppl. 1):S79–87.
- 20 Ahmad I, Fasihullah Q, Noor A, Ansari IA, Ali QN. Photolysis of riboflavin in aqueous solution: a kinetic study. *Int J Pharm* 2004;280:199–208.
- 21 Davies KJ, Delsignore ME, Lin SW. Protein damage and degradation by oxygen radicals. II. Modification of amino acids. *J Biol Chem* 1987;262:9902–07.
- 22 Joshi PC. Ultraviolet radiation-induced photodegradation and ¹O₂, O₂... Production by riboflavin, lumichrome and lumiflavin. *Indian J Biochem Biophys* 1989;26:186–9.
- 23 Davies KJ, Delsignore ME. Protein damage and degradation by oxygen radicals. III. Modification of secondary and tertiary structure. *J Biol Chem* 1987;262:9908–13.
- 24 Morimoto S, Hatta H, Fujita S, Matsuyama T, Ueno T, Nishimoto S. Hydroxyl radical-induced cross-linking of thymine and lysine: identification of the primary structure and mechanism. *Bioorg Med Chem Lett* 1998;8:865–70.
- 25 Joshi PC, Keane TC. Investigation of riboflavin sensitized degradation of purine and pyrimidine derivatives of DNA and RNA under UVA and UVB. *Biochem Biophys Res Commun* 2010;400:729–33.
- 26 Yamamoto F, Nishimura S, Kasai H. Photosensitized formation of 8-hydroxydeoxyguanosine in cellular DNA by riboflavin. *Biochem Biophys Res Commun* 1992;187:809–13.
- 27 Uehara K, Hayakawa T. Photosensitized degradation of guanosine 5'-phosphate by riboflavin. *J Biochem* 1971;70:873–6.
- 28 Uehara K, Hayakawa T. Photooxidation of adenine and its nucleotides in the presence of riboflavin. IV. Photochemical reaction and photoproducts of NAD. *J Biochem* 1972;71:401–15.
- 29 Montana MP, Massad WA, Criado S, Biasutti A, Garcia NA. Stability of flavonoids in the presence of riboflavin-photogenerated reactive oxygen species: a kinetic and mechanistic study on quercetin, morin and rutin. *Photochem Photobiol* 2010;86:827–34.
- 30 Edwards AM, Silva E, Jofre B, Becker MI, De Ioannes AE. Visible light effects on tumoral cells in a culture medium enriched with tryptophan and riboflavin. *J Photochem Photobiol B Biol* 1994;24:179–86.
- 31 Silva E, Barrera M. The riboflavin-sensitized photooxidation of horseradish apoperoxidase. *Radiat Environ Biophys* 1985;24:57–61.
- 32 Jernigan HM, Jr. Role of hydrogen peroxide in riboflavin-sensitized photodynamic damage to cultured rat lenses. *Exp Eye Res* 1985;41:121–9.
- 33 Reiter RJ. Oxidative processes and antioxidative defense mechanisms in the aging brain. *Faseb J* 1995;9:526–33.